Optics and Lasers in Engineering 81 (2016) 113–118

Contents lists available at ScienceDirect

Optics and Lasers in Engineering

journal homepage: www.elsevier.com/locate/optlaseng

Displacement measurement system for inverters using computer micro-vision

Heng Wu [a], Xianmin Zhang [a,*], Jinqiang Gan [a], Hai Li [a], Peng Ge [b,c]

[a] Guangdong Provincial Key Laboratory of Precision Equipment and Manufacturing Technology, School of Mechanical and Automotive Engineering, South China University of Technology, Guangzhou 510640, China
[b] Engineering Research Center for Optoelectronics of Guangdong Province, School of Physics and Optoelectronics, South China University of Technology, Guangzhou 510640, China
[c] Zhejiang Key Discipline of Instrument Science and Technology, China Jiliang University, 310018, China

ARTICLE INFO

Article history:
Received 8 July 2015
Received in revised form
27 December 2015
Accepted 27 December 2015
Available online 12 February 2016

Keywords:
Micro-vision
Image processing
Microscopy
Displacement measurement

ABSTRACT

We propose a practical system for noncontact displacement measurement of inverters using computer micro-vision at the sub-micron scale. The measuring method of the proposed system is based on a fast template matching algorithm with an optical microscopy. A laser interferometer measurement (LIM) system is built up for comparison. Experimental results demonstrate that the proposed system can achieve the same performance as the LIM system but shows a higher operability and stability. The measuring accuracy is 0.283 μm.

1. Introduction

Compliant mechanisms, owing to advantages of simple structure, no friction or wear, high precision, long life and so on, play a significant role in the design of micro-mechanical structures for micro-electro-mechanical systems [1,2]. It has attracted many attentions in recent years. Topology optimization is a basic approach for the design of compliant mechanisms [2]. Generally, in order to investigate the performance of the topology optimization in a quick and direct way, displacement inverters are used [1–7]. During the past few years, displacement inverters have become a typical example in the topology optimization. Zhu et al. presented a two-step elastic modeling method for topology optimization of the compliant mechanisms and the displacement inverters were taken as major numerical examples [2]. Ramrakhyani et al. utilized the displacement inverter problem to demonstrate the effectiveness of the elements which were designed by the topology design [3]. Saxena et al. used the displacement inverter as synthesis examples to verify the structural property [4]. In addition, Kim et al. [5], Ansola et al. [1] and so on [6–8] employed the displacement inverters to check performance of their designs. With rapid developments of compliant mechanism design, the displacement inverters will be more widely used in the future. Since the displacement inverters are usually small and thin, and constructed by special grids [1–8], it is a challenging work to detect their displacements.

The LIM is one of the widely used methods to measure the displacements of the inverters. The measurement accuracy can reach to nanoscale. However, environmental conditions such as humidity, air temperature and pressure, usually bring interference to the measuring results even though a precision stabilized laser source and accurate environmental compensation are utilized. Moreover, a reflecting device is needed to be mounted on the inverter. It is not convenient when the inverter's grids are too big or beam elements are too small. The weight of the reflecting device may also cause deformation to the inverter, which can affect the measurement accuracy. Hsieh et al. introduced a grating-based interferometer for six degrees of freedom displacement and angle measurement [9]. The system of their method is complex and inconvenient for the general use. Berkovic et al. recommended many optical methods for distance and displacement measurements [10]. Some other researchers such as Cofaru et al. [11], Mudassar et al. [12] and Yuan et al. [13] developed image processing techniques and vision-based techniques for displacement measurements. Both a strong robustness and high accuracy are achieved by these techniques and the system setups are quite simple.

To the best of our knowledge, few literatures have been presented for the displacement measurement of the inverters utilizing the computer micro-vision in the compliant mechanism

* Corresponding author.
E-mail address: zhangxm@scut.edu.cn (X. Zhang).

http://dx.doi.org/10.1016/j.optlaseng.2015.12.018

design. In this paper, we describe a practical system for the displacement measurement of the inverters using the micro-vision-based technology, which can acquire a high accuracy. The setup of the proposed system is much simpler and cheaper than the LIM system, but the accuracy of the proposed system is the same as the LIM system and the operability and stability of the proposed system are much higher. This system can give a great help for the compliant mechanism design.

2. Methodology

The system setup is sketched in Fig. 1 and the actual experimental setup of the system is shown in Fig. 2. The whole workstation includes an inverter in combination with a piezoelectric translator (PZT) driver system, a PC and an imaging system. The PZT is a stack piezoelectric translator PST 150/7/60VS12, which is a preloaded PZT from Piezomechanik in Germany. The PZT is installed inside the inverter which is mounted on a vibration-free positioning platform. The imaging system consists of an optical microscope with a controllable zoom (magnification from 0.71 × to 4.5 ×), and a CCD camera (JAI CV-A2, black and white) with a resolution of 1500 × 1200. The pixel size of the CCD camera is 4.4 μm. A 10 × objective is used, which has a depth of field of 3.5 μm. During the experiment, the total magnification of the system is 15.54 × . The pixel space of the CCD camera is $C_x = C_y = 0.283$ μm/pixel.

The displacement measurement process of the proposed system, which is based on the template matching, is composed of a coarse search and a fine search. The coarse search is to find out the potential regions that the centroid point of the template might be in. The fine search is to determine the accurate location of the template in the reference images. Let $I(x, y)$ denote the intensity value of the image I with the size $M \times N$ at the point (x,y),$x\in\{1,\ldots,M\}$, $y\in\{1,\ldots,N\}$. Similarly, let $T(x,y)$ be the intensity value of the $m \times n$ template T at the point (x,y) where $m \le M$ and $n \le N$. In order to determine the potential regions, a testing function for evaluating the error between the template and the candidate image is defined as Eq. (1) [14],

$$\varepsilon(x_k, y_k, i, j) = \left|I(x_k+i, y_k+j) - T(x_k, y_k) - \bar{I}(i,j) + \bar{T}\right|, \tag{1}$$

where (x_k, y_k) represents the randomly selected coordinate which is nonrepeating, $k = 1, 2, \cdots, m \times n$, $i = 1, 2, \cdots, M-m+1$, $j = 1, 2, \cdots, N-n+1$, $\bar{I}(i,j)$ and $\bar{T}$ are the average gray-scale values of the reference and the template image, respectively, which are

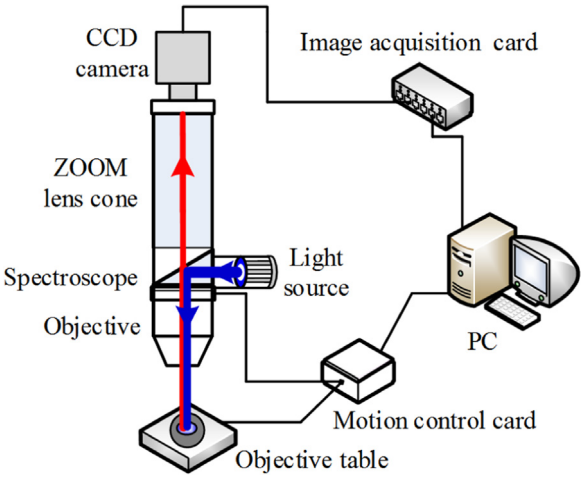

Fig. 1. The sketch map of the measuring system.

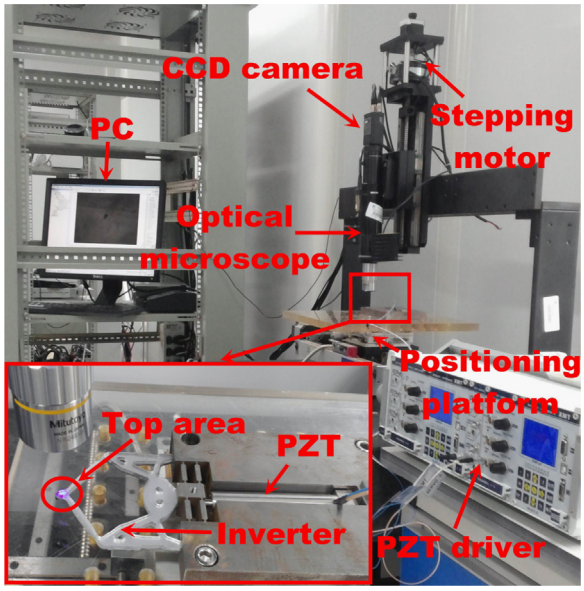

Fig. 2. The experimental setup of the micro-vision system.

expressed as follows:

$$\bar{I}(i,j) = \frac{1}{m \times n} \sum_{x=1}^{m} \sum_{y=1}^{n} I(x+i, y+j), \tag{2}$$

$$\bar{T} = \frac{1}{m \times n} \sum_{x=1}^{m} \sum_{y=1}^{n} T(x,y). \tag{3}$$

Then, a constant threshold T_{thr} is employed to test the accumulated errors as shown in Eq. (1). If the accumulated error exceeds T_{thr}, the calculation is stopped and the point (i,j) and the test number d are recorded, else the calculation will go on until $k = m \times n$. The surface detection function $S(i,j)$ is expressed as

$$S(i,j) = \left\{ d \left| \min_{1 \le d \le m \times n} \left[\sum_{k=1}^{d} \varepsilon(x_k, y_k, i, j) \ge T_{thr} \right] \right. \right\}. \tag{4}$$

When the value of $S(i,j)$ where the accumulated error exceeds T_{thr} are acquired, the corresponding points are considered as potential points. Then, each potential point is set as the centroid point of a corresponding square which is created with a side length L, where L represents the number of pixels. The squares are regarded as the potential regions. Unlike traditional template matching algorithms where the upper left point is usually taken as the reference point, the centroid point is selected as the reference point of the template in our algorithm, which is presented as

$$x = \frac{\sum_{x=1}^{m} \sum_{y=1}^{n} x \cdot T(x,y)}{\sum_{x=1}^{m} \sum_{y=1}^{n} T(x,y)}, \quad y = \frac{\sum_{x=1}^{m} \sum_{y=1}^{n} y \cdot T(x,y)}{\sum_{x=1}^{m} \sum_{y=1}^{n} T(x,y)}. \tag{5}$$

After that, the normalized cross-correlation (NCC) algorithm is used to calculate the precise location from the potential regions in the image. The computation process is repeated for every point in the potential regions and the NCC coefficient value is recorded correspondingly. The point with the highest score is selected as the final point. The NCC coefficient is defined as

$$R(i,j) = \frac{\sum_{x=1}^{m} \sum_{y=1}^{n} I(x+i, y+j) \cdot T(x,y) - m \cdot n \cdot \bar{I}(i,j) \cdot \bar{T}}{\sqrt{\sum_{x=1}^{m} \sum_{y=1}^{n} I^2(x+i, y+j) - m \cdot n \cdot \bar{I}^2(i,j)} \cdot \sqrt{T_C}}, \tag{6}$$

where T_C is a constant which is denoted as

$$T_C = \sum_{x=1}^{m}\sum_{y=1}^{n}(T(x,y)-\overline{T})^2. \quad (7)$$

To accelerate the calculation speed, the sum-tables are employed [15]. When the final point is obtained, the new position of the centroid point is expressed as

$$x'_u = (x_u - x_0)\cdot C_x,\ y'_u = (y_u - y_0)\cdot C_y, \quad (8)$$

wherein x_u and y_u, x_0 and y_0 specify the new and original pixel coordinates of the template in the reference image coordinate system, respectively, and u signifies the detecting numbers.

3. Experiments and analysis

Since the motion range of the inverter is less than 1 mm, the top area of the inverter is used for testing as shown in Fig. 3(a). As the inverter has only one degree of freedom in this experiment, the displacement measurement along the x-axis is concerned. Fig. 3(b) shows the top area of the inverter in the CCD camera when the PZT power is off. A feature part is cut as the template. To guarantee the template is always in the field of the view, we select the feature part which is around the center of the reference image as the template. Then the centroid point of the template is set as the origin of the Cartesian coordinate system.

After that, the PZT is controlled to output the displacements within the range of 0–45 μm, and the centroid point position of the template in the reference image is correspondingly calculated. Twenty group experiments are carried out and 10 figures are captured in each group. Fig. 4 shows experimental results. It can be seen from Fig. 4(a) that the displacement curves are consistent with each other. Fig. 4(b) shows the relative displacement which is defined as the difference between the input displacement and the output displacement. A few deviations among the curves are caused by the matching algorithm whose positional accuracy is an integral pixel. As the motion range of the inverter is in the micron scale, the single pixel deviation (0.283 μm) can be accepted.

To compare the performances with other professional measuring equipment, a high-precision LIM system is established. The system setup is shown in Fig. 5. The laser interferometer is Renishaw XL-80 which has a linear measurement accuracy of ± 0.5 ppm, a maximum linear measurement speed of 4 m/s and a

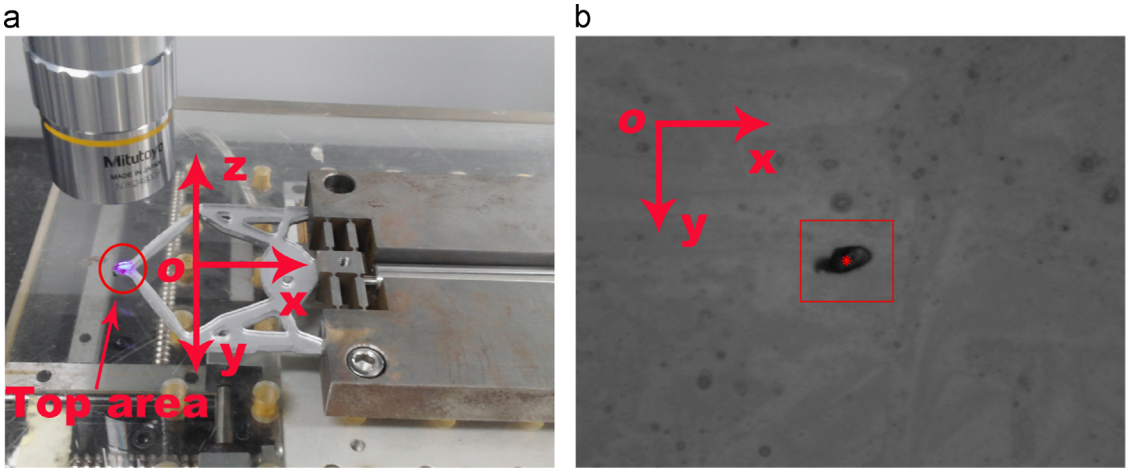

Fig. 3. The selection of the template.

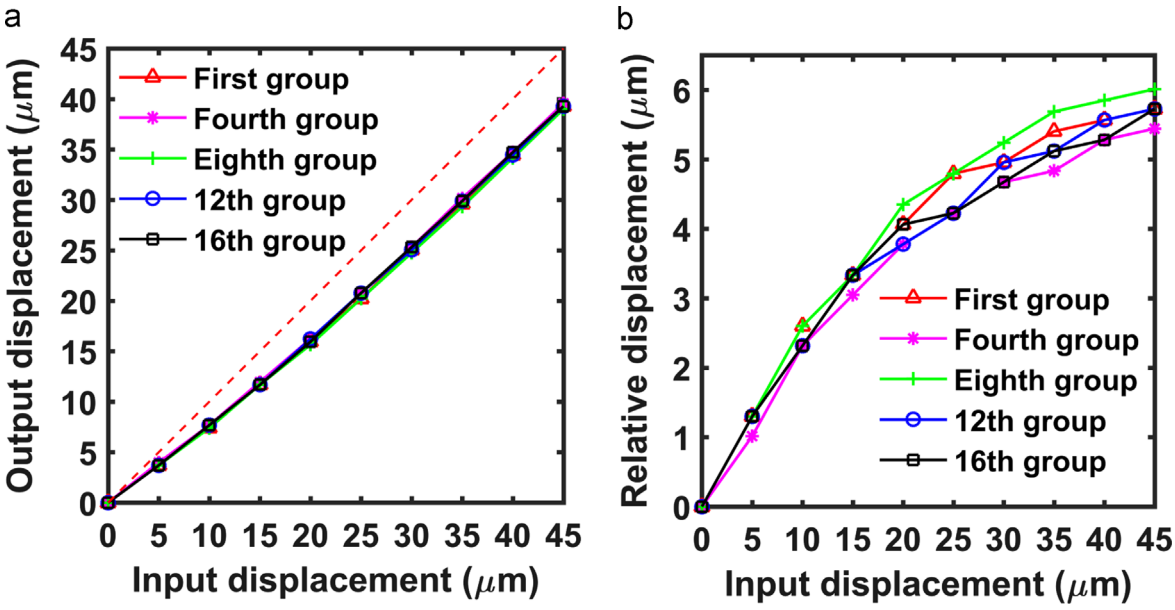

Fig. 4. Experimental results by the proposed method.

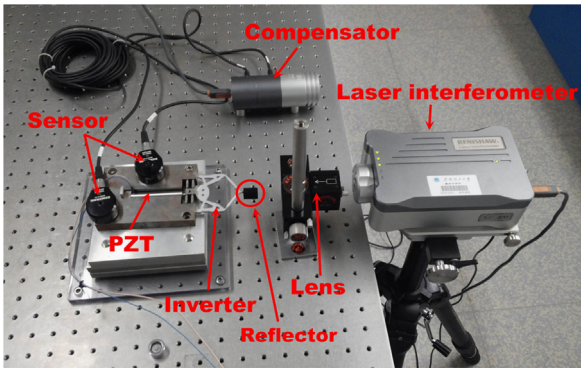

Fig. 5. The experimental setup of the LIM system.

linear resolution of 1 nm even at the maximum speed. The measuring results are presented in Fig. 6(a), where the displacement curves coincide with each other well. Fig. 6(b) displays the relative displacements at each test group. Few deviations are generated which means a high accuracy is achieved.

Fig. 7(a) shows the average values of measurements at the relative points by the LIM system and the proposed system. Fig. 7 (b) exhibits the average relative displace-ments by the two systems. We can find that the deviations between the two systems are small. The residual errors produced by the laser interferometer measurements and the proposed system are shown in Fig. 8. Here, the residual error is defined as the difference between the test value and the average value of test values. It can be seen the deviation fluctuations of our system are much larger than the LIM

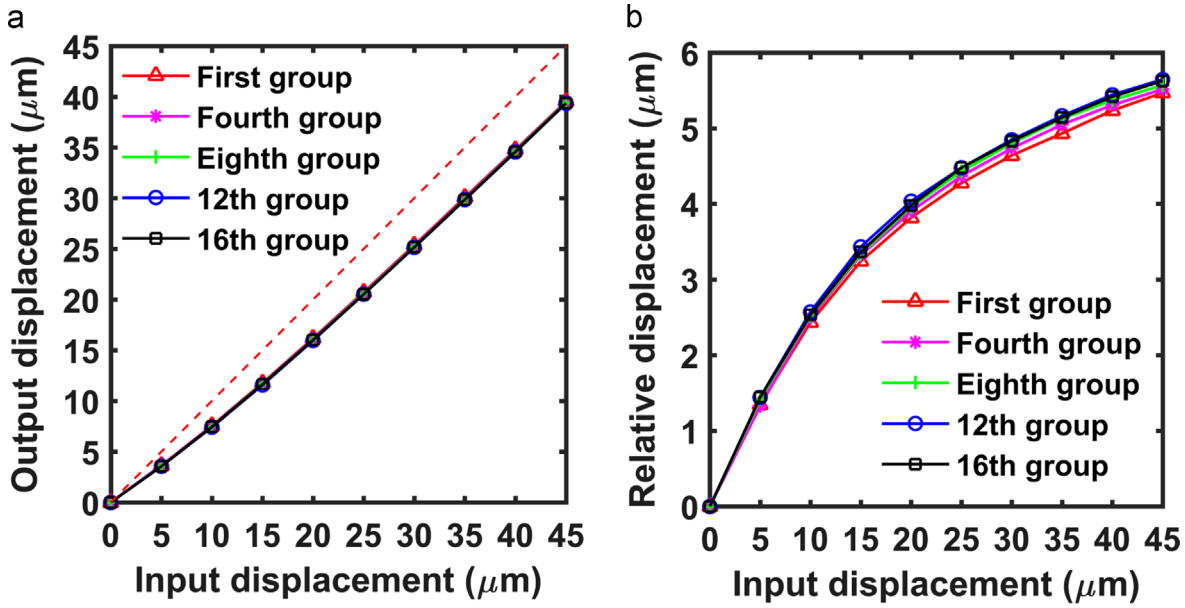

Fig. 6. Experimental results by the laser interferometer measurements.

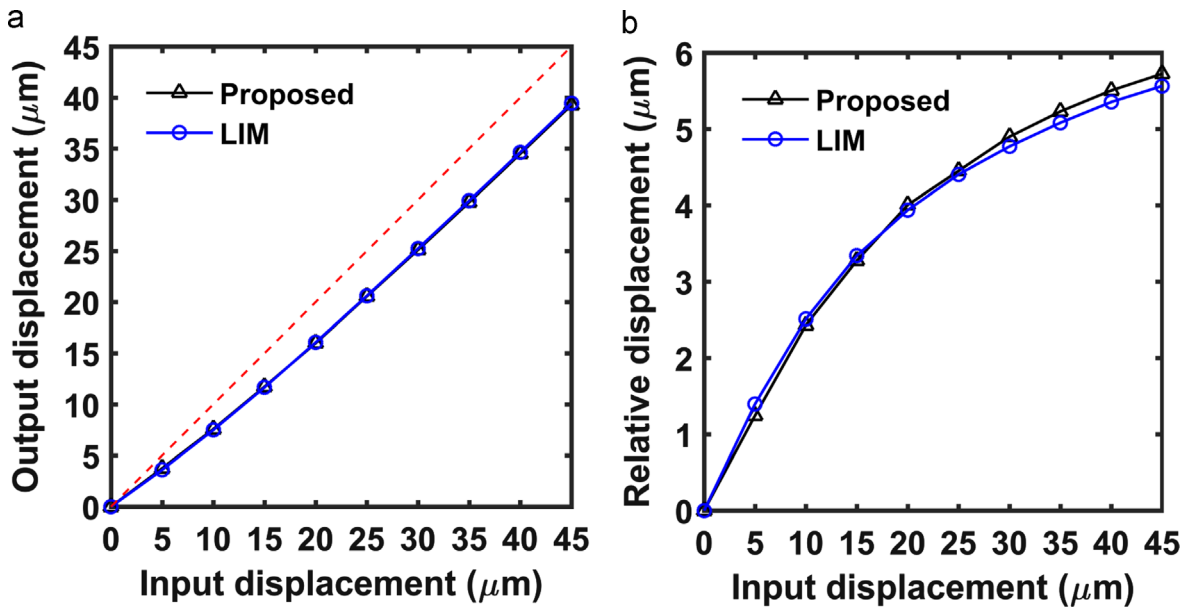

Fig. 7. Average value comparisons between the proposed method and the laser interferometer measurements.

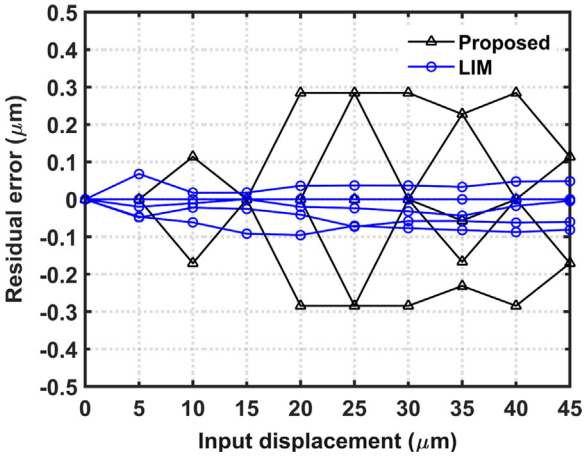

Fig. 8. Residual error comparisons between the proposed method and the laser interferometer measurements.

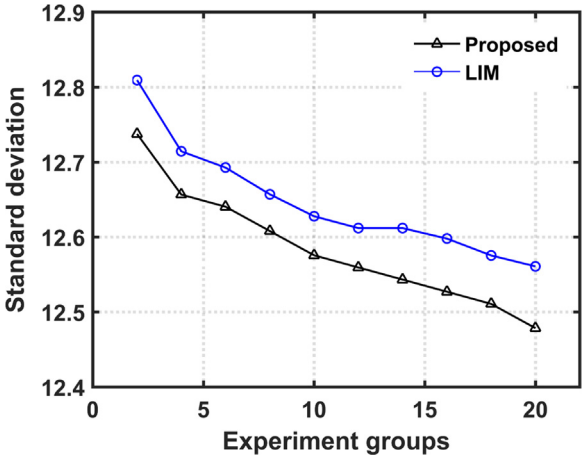

Fig. 9. Standard deviation comparisons between the proposed method and the laser interferometer measurements.

system, and the deviations have a symmetrical distribution. The main reason is the single-pixel positional accuracy of the matching algorithm. The system and environmental noises also put some influences on the measuring results. The different deviation values in Fig. 8 are caused by the computing processes of residual errors. Fig. 9 shows the experimental standard deviations of the two systems. Although our system has a larger residual error, the experimental standard deviation at each group is smaller than the laser interferometer measurements. This indicates that the results of our system are more stable as the measuring groups increase. As the deviations between the two systems are small, it means that the experiments are taken in an accurate and reliable way. From the experimental results, we can find that our system shows a good consistency with the LIM. Although some small deviations appear compared with the LIM system, the measuring results are satisfied. Moreover, as shown in Figs. 2 and 5, it can be seen that the setup of our system is simpler than the LIM system and the measuring result are more stable than the LIM system. That means our system has a higher operability and stability.

4. Conclusions

In this paper, a practical system of the displacement measurements for the inverters using the computer micro-vision at the sub-micron scale is proposed. With this system, the displacement measurement is converted into a fast template matching problem for the image processing. Experimental results demonstrate that the proposed system can replace traditional measuring tools in some special occasions where the traditional ones cannot manage well. As the template matching algorithm is based on the integral pixels, the minimum resolution of the proposed method is only a pixel. The sub-micron spatial resolution of the proposed system is actually owing to the high resolution of the optical microscope and the CCD camera. If a higher magnification objective is adopted or the sub-pixel algorithms are employed, the nanoscale resolution can be achieved. Moreover, although one dimensional displacement is measured in this paper, the algorithm, which is realized by the one camera methodology, is fundamentally two-dimensional (2D). It is well capable of measuring in-plane displacements. Any out-of-plane displacements will lead to the measurement errors. In addition, since the magnification of the optical microscope is high and the depth of field of the objective is small, the *Z* direction motion can induce high pseudo in-plane motion in the image plane and make the image become blurred, which will damage the measurements. Thus, it is necessary to develop the three-dimensional (3D) displacement measurement methods.

Although it is not presented in this paper, the proposed method possesses the potential capability of 3D displacement measurements. Furthermore, the proposed system uses only low-cost elements and it can be used not only for the displacement measurement, but also for the surface defect detection, the micro-motion detection and so on. Future studies will focus on the following aspects. First, the application of 2D methods to 3D situations should be investigated. Second, the nanoscale 3D displacement measurements and object visualization in the proposed system need to be experimentally demonstrated.

Acknowledgments

This work was supported by the Scientific and Technological Project of Guangzhou (Grant no. 2015090330001), the National Natural Science Foundation of China (Grant nos. 91223201 and U1501247), the Natural Science Foundation of Guangdong Province (Grant nos. S2013030013355 and 2015A030310278), the Fundamental Research Funds for the Central Universities (2012ZP0004 and 2015ZZ131), Zhejiang Key Discipline of Instrument Science and Technology, Zhejiang Key Lab of Flow Measurement (Grant no. JL150510), and Supported by Hunan Province Key Laboratory of Videometric and Vision Navigation.

References

[1] Ansola Rubén, Veguería Estrella, Canales Javier, Tárrago José A. A simple evolutionary topology optimization procedure for compliant mechanism design. Finite Elem Anal Des 2007;44(1):53–62.
[2] Zhu Benliang, Zhang Xianmin, Fatikow Sergej. Level set-based topology optimization of hinge-free compliant mechanisms using a two-step elastic modeling method. J Mech Des 2014;136(3):031007.
[3] Ramrakhyani Deepak S, Frecker Mary I, Lesieutre George A. Hinged beam elements for the topology design of compliant mechanisms using the ground structure approach. Struct Multidiscip Optim 2009;37(6):557–67.
[4] Saxena A, Ananthasuresh GK. On an optimal property of compliant topologies. Struct Multidiscip Optim 2000;19(1):36–49.
[5] Kim Jae Eun, Kim Yoon Young, Min Seungjae. A note on hinge-free topology design using the special triangulation of design elements. Commun Numer Methods Eng 2005;21(12):701–10.
[6] Pedersen Claus BW, Buhl Thomas, Sigmund Ole. Topology synthesis of large-displacement compliant mechanisms. Int J Numer Methods Eng 2001;50(12):2683–705.
[7] Zhou Hong. Topology optimization of compliant mechanisms using hybrid discretization model. J Mech Des 2010;132(11):111003.
[8] Sigmund Ole. On the design of compliant mechanisms using topology optimization. J Struct Mech 1997;25(4):493–524.

[9] Hsieh Hung-Lin, Pan Ssu-Wen. Development of a grating-based interferometer for six-degree-of-freedom displacement and angle measurements. Opt Express 2015;23(3):2451–65.
[10] Berkovic Garry, Shafir Ehud. Optical methods for distance and displacement measurements. Adv Opt Photonics 2012;4(4):441–71.
[11] Cofaru Corneliu, Philips Wilfried, Paepegem Wim Van. Pixel-level robust digital image correlation. Opt Express 2013;21(24):29979–99.
[12] Mudassar Asloob Ahmad, Butt Saira. Improved digital image correlation for in-plane displacement measurement. Appl Opt 2014;53(5):960–70.
[13] Yuan Yuan, Huang Jianyong, Fang Jing, Yuan Fan, Xiong Chunyang. A self-adaptive sampling digital image correlation algorithm for accurate displacement measurement. Opt Lasers Eng 2015;65:57–63.
[14] Barnea Daniel I, Silverman Harvey F. A class of algorithms for fast digital image registration. IEEE Trans Computers 1972;C-21:179–86.
[15] Lewis JP. Fast normalized cross-correlation. Vis Interface 1995;10(1):120–3.